ISBN: 978-3-95450-184-7 doi:10.18429/JACoW-IPAC2018-THPAK139

LOST MUON STUDIES FOR THE MUON g-2 EXPERIMENT AT FERMILAB*

S. Ganguly†, K. T. Pitts, University Of Illinois At Urbana-Champaign, Urbana, United States of America
J. D. Crnkovic, Brookhaven National Laboratory, Upton, United States of America
C. C. Polly, Fermi National Accelerator Laboratory, Batavia, United States of America
on behalf of the Muon g-2 Collaboration

Abstract

The Fermilab Muon g-2 experiment aims to measure the muon anomalous magnetic moment a_μ with an unprecedented precision of 140 parts per billion (ppb), a four-fold improvement over the 540 ppb precision obtained by the BNL Muon g-2 experiment. This study presents preliminary work on estimating the muon losses by using double coincidences in the calorimeters.

INTRODUCTION

The muon magnetic moment is related to the muon spin via a dimensionless proportionality constant known as the muon g-factor (g). Dirac theory predicts that $g = 2$ for spin-1/2 point particles such as the muon, while Standard Model (SM) Quantum Field Theory predicts that $g \neq 2$. The fractional deviation of g from 2 is known as the magnetic anomaly. The final Brookhaven National Laboratory (BNL) muon a measurement [1] is

$$a_\mu \equiv \frac{g-2}{2} = 116\,592\,091\ (54)\,(33) \times 10^{-11}, \qquad (1)$$

with statistical and systematic errors quoted respectively within the parentheses. The BNL measurement has a more than 3σ difference [1, 2] from the SM prediction, indicating the possibility of physics beyond the SM. The Fermi National Accelerator Laboratory (Fermilab) Muon g-2 experiment has the goals of increasing the statistics by more than a factor of 20 and reducing systematic errors by a factor of 3.

The Fermilab Muon Campus [3] produces a high intensity and highly polarized muon beam that is injected into the storage ring. The muon beam is injected into the storage ring via the inflector magnet which is designed to minimize perturbations to the very uniform storage ring magnetic field. Fast magnetic kickers transfer the injected off orbit muons onto the central orbit. The Fermilab Muon g-2 experiment uses 24, 6×9 segmented PbF_2 Cherenkov crystal calorimeters [4, 5] which measure decay positron energy and arrival time. The muon anomaly can be determined by a precise measurement of the muon spin precession ω_a in the storage ring and the magnetic field B. When excluding systematic effects, the decay positron counts (N) can be described by a 5-parameter fit function [6, 7],

$$N(t) = (N_0/\tau) * e^{-t/\tau}[1 - A\cos(\omega_a t + \phi)], \qquad (2)$$

where t is the arrival time of the positrons from the muon decays, N_0 is normalization, τ is the lab-frame muon lifetime, A is asymmetry, and ϕ is the intial phase of the muon polarization. Muons at the edge of the phase space are favorably lost at early times, leading to a deviation from pure exponential muon decay in Eq. 2. The average spin of the lost muons can differ from that of the fully stored muons, if these 2 muon populations are created at different points in the production beamline. This difference in average spin phase can cause a shift in the measured ω_a. The Fermilab experiment has a goal of keeping the relative number of lost muons below 10^{-4} per τ.

The Fermilab Muon g-2 experiment is currently in the first physics data taking run. This discussion presents lost muon studies based on preliminary experimental data that uses double coincident events in the calorimeters. These studies were in part used to avoid muon storage ring betatron resonances [8] when establishing the voltages for the electrostatic quadrupole system (EQS) that provide vertical focusing and determine the n-value for the storage ring dynamics.

DETECTION OF LOST MUONS

The BNL experiment measured lost muons by searching for three-fold coincidences in consecutive calorimeters. The energy deposited by MIPs were far below the hardware threshold of the calorimeters used by the BNL experiment. The BNL experiment used scintillator detectors mounted on the front of the calorimeters. Thanks to better calorimeter segmentation and timing precision, the Fermilab experiment is developing lost muon measurement techniques based on either two or three-fold coincidences in consecutive calorimeters. This discussion only covers lost muon detection techniques using two-fold coincidences. The red line shows an example decay electron trajectory while the blue line shows a lost muon trajectory. Two detection coincidences in adjacent calorimeters are used to select muon candidates, where the calorimeters are located every 15° around the storage ring. The 3 GeV lost muons typically

* We thank William M. Morse for his advice and guidance. This document was prepared by the Muon g-2 Collaboration using the resources of the Fermi National Accelerator Laboratory (Fermilab), a U.S. Department of Energy, Office of Science, HEP User Facility. Fermilab is managed by Fermi Research Alliance, LLC (FRA), acting under Contract No. DE-AC02-07CH11359. This manuscript has been authored by the employees of University of Illinois at Urbana-Champaign, supported by the U.S. Department of Energy, grant DE-SC0015640.
† sgang28@illinois.edu

ISBN: 978-3-95450-184-7 doi:10.18429/JACoW-IPAC2018-THPAK139

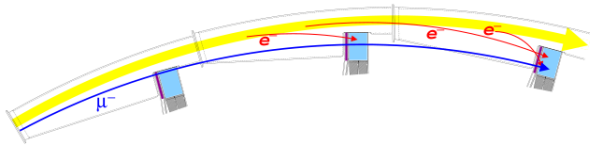

Figure 1: Diagram [6] of a lost muon detected by finding three-fold coincidences among three consecutive calorimeters. The red line shows example decay electron trajectories while the blue line shows a lost muon trajectory.

correspond to a MIP (minimum ionizing particle) that deposits ~ 170 MeV into a calorimeter crystal when passing through it, unlike the decay positrons which typically produce an electromagnetic shower that deposits almost all of the energy into the calorimeter. These two distinct behaviors allow for the isolation of lost muons. However, low energy decay positrons can produce a MIP-like signature leading to a source of background. A muon typically takes 6.25 ± 0.5 ns (time-of-flight) to travel from one calorimeter to the next calorimeter depositing MIP-like energies in a single crystal in each calorimeter. Unlike the muon events, decay positron events tend to deposit energy across multiple crystals. Also a muon candidate tends to curl inwards (away from the ring) while going from the first calorimeter to the next one where the decay positrons are more abundant near the storage ring. The low energy decay positrons contribute to two types of backgrounds to the lost muon signal: uncorrelated two low energy e^+ backgrounds (random coincidences occurring when two independent decay positrons or a second lost muon are randomly detected in the coincidence time window) and correlated single e^+ background where a single e^+ can pre-shower and deposit MIP-like energies in two consecutive calorimeters. Figure 1 shows the detection of a lost muon through three-fold coincidences among three consecutive calorimeters. Using the unique behaviors of the muons vs decay positrons a cut-based analysis has been performed using a MC simulation of the beam originating at the inflector exit and the same cuts have been applied later to extract the loss function from two-fold coincidences using experimental data.

A muon cluster is formed by calculating energy weighted position and time (as given by Eq. 3) of the crystal hits in a calorimeter:

$$(X,Y,t) \quad = \quad \left(\sum E_{xtal} \times (X,Y,t)_{xtal}\right) \Big/ \sum E_{xtal} \ . \tag{3}$$

Three selections [9] have been used to reduce correlated single e^+ backgrounds:

1. $E_{frac} = E_{max}/E_{total} > 0.8$.
2. Spatial distance between the cluster centers in two consecutive calorimeters $X_2 - X_1 < 0$.
3. Number of crystal hits in a cluster < 3.

Cut (1) shows the fraction energy in a cluster where E_{max} is the maximum energy in a a single crystal and E_{total} is the total energy in that cluster. Cut (1) provides a good lost muon signal selection as E_{frac} should be ~1 for muon candidates. Cut (2) removes the positrons side-entering into the adjacent calorimeter therefore mostly hitting the crystals closest to the storage volume. Cut (3) removes background decay positrons as they produce electromagnetic shower hitting more crystals in a cluster compared to the muons hitting fewer than three crystals. Figure 2 shows the azimuthal distribution of the lost muon signal with > 30 μs after applying the above-mentioned cuts. The EQS scraping [7] reduces

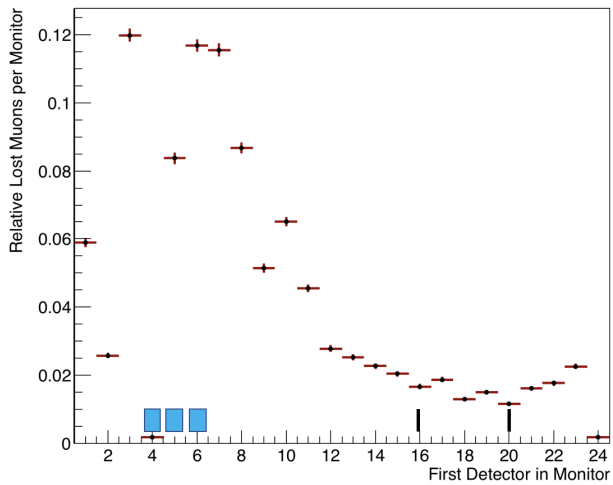

Figure 2: Preliminary results showing the azimuthal distribution of lost muons observed by detectors placed around the storage magnet. The variation in the azimuthal muon losses observed by detectors is a complicated mix of geometrical and detector MIP-detection efficiencies coupled with the underlying muon loss mechanism and placement of collimators in the ring. The area under the curve is normalized to unity. The black lines show the locations of the collimators, and the cyan bars show the location of the kicker plates.

lost muons during the measurement period. The storage ring horizontal and vertical tunes are effectively determined by the EQS operating voltages [7, 10]. Storage ring betatron resonances increase the number of lost muons, and so it is desirable to find EQS operating voltages that avoid the large betatron resonances. Figure 3 shows a scan of lost muons per decay electron in the first calorimeter and with energy > 1.8 GeV as a function EQS storage set-point voltage. A large increase in lost muons is clearly seen from the betatron resonances centered near 18.8 and 21.2 kV. These data were taken without beam scraping, and corresponding decreases in the number of observed decay e^+ are also seen near these EQS storage set-point voltages [8].

ISBN: 978-3-95450-184-7 doi:10.18429/JACoW-IPAC2018-THPAK139

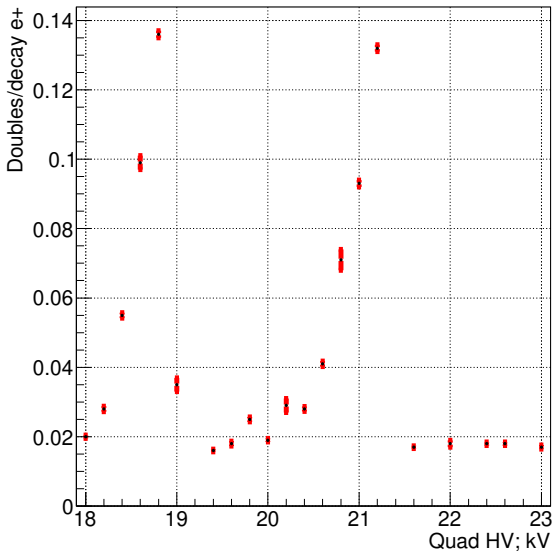

Figure 3: Fraction of lost muons as a function of EQS storage set-point voltage for calorimeter 1. An increased lost muon rate is observed from the betatron resonances centered near 18.8 and 21.2 kV. These resonances are due to $3Q_y = 1$ and $Q_x + 2Q_y = 2$ line in the tune plane.

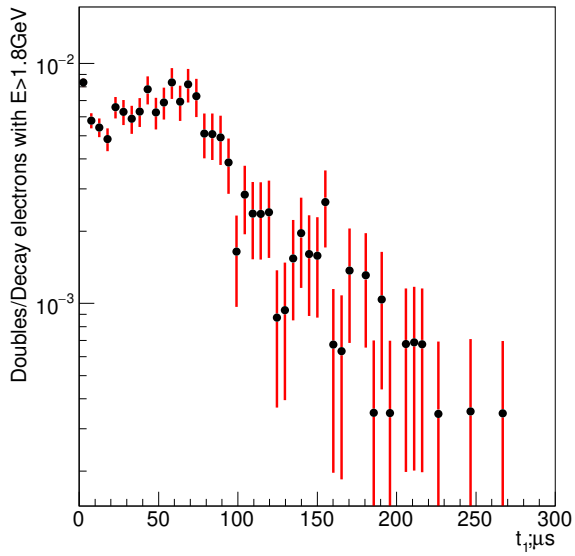

Figure 4: $L(t)$ from double coincidences for calorimeter 1.

CONSTRUCTION OF THE LOSS FUNCTION

Figure 4 shows the loss function ($L(t)$) providing the rate at which muons are lost from the ring as a function of time after injection, constructed from double coincidences. The losses are normalized with a pure exponential with the expected lifetime of 64.4 μs and an amplitude determined from the number of decay electrons with energies > 1.8 GeV measured in the first calorimeter in a double coincidence. The ratio of lost muons to decay positrons is expected to be much higher at early times than at late times. The loss function ($\Lambda(t)$ [6]) is a correction factor to N_0 (see Eq. (2)) that accounts for muon losses.

$$\Lambda(t) = 1 - Ce^{-t_0/\tau} \int_{t_0}^{t} (L(t'))e^{t'/\tau} dt',$$

where the integral can be evaluated numerically with τ = 64.4 μs, t_0 is the canonical fit start time and the parameter C is allowed to float in the fit, thereby including a sixth parameter into Eq. 2.

Figure 5 shows an example of the loss function using data integrated over t_0 = 30 μs to t = 300 μs.

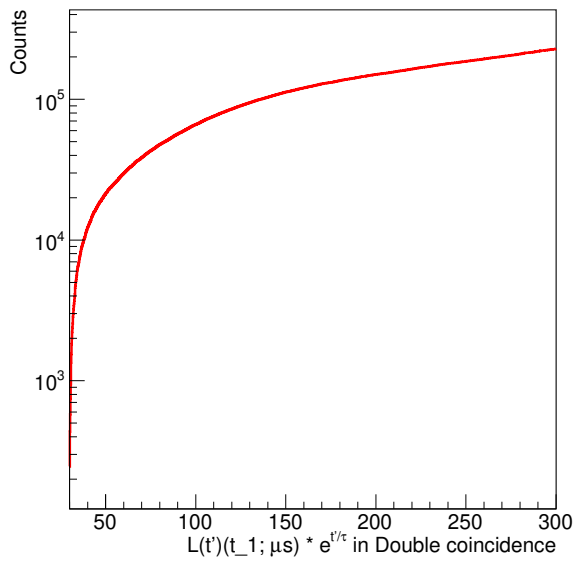

Figure 5: Loss function from double coincidence for calorimeter 1, integrated over t_0 = 30 μs to t = 300 μs.

CONCLUSION

The Fermilab Muon g-2 experiment is currently in the first physics data taking phase. Lost muon systematic effects causes a systematic effect on ω_a when extracting from the 5-parameter fit. MC simulation of the muon beam and storage ring has been used to optimize the lost muon signal by taking advantage of highly segmented calorimeters to distinguish the lost muons from the much larger decay positron backgrounds. Preliminary physics data have been used to determine electrostatic quadrupole operating voltages by looking at fractional muon losses and estimate the rate of losses over time using double coincidence calorimeter events.

ISBN: 978-3-95450-184-7 doi:10.18429/JACoW-IPAC2018-THPAK139

REFERENCES

[1] C. Patrignani *et al.* (Particle Data Group), Chin. Phys. C **40**, 100001 (2016) and 2017 update.

[2] T. Blum, A. Denig, I. Logashenko, E. de Rafael, B. Lee Roberts, T. Teubner and G. Venanzoni, arXiv:1311.2198 [hep-ph].

[3] D. Stratakis *et al.*, *Phys. Rev. Accel. Beams* **20**, no. 11, 111003 (2017) doi:10.1103/PhysRevAccelBeams.20.111003 [arXiv:1803.00597 [physics.acc-ph]].

[4] A. T. Fienberg *et al.*, *Nucl. Instrum. Meth. A* **783**, 12 (2015) doi:10.1016/j.nima.2015.02.028 [arXiv:1412.5525 [physics.ins-det]].

[5] J. Kaspar *et al.*, *JINST* **12**, no. 01, P01009 (2017) doi:10.1088/1748-0221/12/01/P01009 [arXiv:1611.03180 [physics.ins-det]].

[6] C. Polly, "A Measurement of the Anoumalous Magnetic Moment of the Negative Muon to 0.7 ppm" Ph.D. thesis, Phys. Dept., The Graduate College of the University of Illinois at Urbana-Champaign, Urbana, Illinois, United States of America, 2005.

[7] G. W. Bennett *et al.* [Muon g-2 Collaboration], *Phys. Rev. D* **73**, 072003 (2006) doi:10.1103/PhysRevD.73.072003 [hep-ex/0602035].

[8] J. D. Crnkovic *et al.*, presented at IPAC'18, Vancouver, Canada, April 2018, paper WEPAF015, this conference.

[9] S. Ganguly, J. D. Crnkovic *et al.*, in *Proc. IPAC'17,* Copenhagen, Denmark, May 2017, paper WEPIK119, pp. 3230–3233.

[10] J. Grange *et al.* [Muon g-2 Collaboration], arXiv:1501.06858 [physics.ins-det].